Fire-after-earthquake resistance of steel structures using rotational capacity limits

Daphne Pantousa[a] and Euripidis Mistakidis[*]

Laboratory of Structural Analysis and Design, Department of Civil Engineering, University of Thessaly, Pedion Areos, Volos, Greece

Abstract. This paper addresses numerically the behavior of steel structures under Fire-after-Earthquake (FAE) loading. The study is focused on a four-storey library building and takes into account the damage that is induced in structural members due to earthquake. The basic objective is the assessment of both the fire-behavior and the fire-resistance of the structure in the case where the structure is damaged due to earthquake. The combined FAE scenarios involve two different stages: during the first stage, the structure is subjected to the ground motion record, while in the second stage the fire occurs. Different time-acceleration records are examined, each scaled to multiple levels of the Peak Ground Acceleration (PGA) in order to represent more severe earthquakes with lower probability of occurrence. In order to study in a systematic manner the behavior of the structure for the various FAE scenarios, a two-dimensional beam finite element model is developed, using the non-linear finite element analysis code MSC-MARC. The fire resistance of the structure is determined using rotational limits based on the ductility of structural members that are subjected to fire. These limits are temperature dependent and take into account the level of the structural damage at the end of the earthquake and the effect of geometric initial imperfections of structural members.

Keywords: Fire-After-Earthquake loading; frame structures; rotational capacity; fire-resistance

1. Introduction

In urban areas Fire-After-Earthquake (FAE) is a rather common case and, occasionally, can be catastrophic. The aftermath of the fire outbreak after an earthquake has many times been witnessed in recent years (Northridge 1994, Kobe 1995, Chile 2010, Tohoku 2011). In many cases, urban environment characteristics (gas piping system, electricity wiring system, etc.) and post-earthquake conditions (multiple ignition points, malfunction of the active fire-protection systems, etc.) are combined and the fire that follows earthquake becomes the predominant cause of damage and loss of human life (Scawthorn *et al.* 2005).

Until now, the post-earthquake fire design is not a normative requirement and the fire design codes assume that when a fire starts, the structure is intact. This is not valid when structures have been damaged due to a prior seismic action. In order to conduct an integrated study for the post-

---

*Corresponding author, Professor, E-mail: emistaki@uth.gr
[a]Dr. Ing., E-mail: dpantousa@gmail.com

earthquake fire performance of structures, the seismic damage of structural components needs to be taken into account. Specifically, considering steel frame structures that are designed according to the ductility requirements of the capacity design rules of Eurocode 8 (2004), it is expected that at the starting point of the fire, the plastic hinges have already been formed (fully or partially) at the ends of the beams.

Moreover, concerning the FAE situations, there exisst extensive literature about the disasters that are attributed to the post-earthquake fires in urban regions. Several studies are devoted to the historical events and indicate the mitigation strategies for the reduction of the post-earthquake fire losses in urban regions. On the other hand, the scientific research on the fire-behaviour of unprotected steel structures has recently been started. The interest mainly lies on the behavior of steel frame buildings under the FAE loading (Faggiano *et al.* 2007, Faggiano *et al.* 2008, Yassin *et al.* 2008, Zaharia *et al.* 2007, Zaharia *et al.* 2008, Zaharia *et al.* 2009, Della Core *et al.* 2003, Keller 2012, Faggiano and Mazzolani 2011, Keller and Pessiki 2012, Kodur and Dwaikat 2009, Zaharia and Pintea 2009, Lee *et al.* 2008, Zhao 2010). In these studies the criteria used for the determination of the fire-resistance time are based on the strength or stability criteria of structural members or on the global stability of the structure. Effects of the earthquake excitation on the criteria used for the determination of the fire-resistance of structures have not yet been considered.

The main problem addressed in the present study is the assessment of the behaviour of steel frame structures at elevated temperatures, considering that the starting point is a state of permanent damage caused by a prior seismic event, using numerical methods. Moreover, the determination of the fire-resistance (in time domain) of structures during post-earthquake fire events is calculated. In this way the fire-resistance calculated depends on the damage caused by earthquake. The study is focused on a steel-frame building that is used as a library. However, the developed methodology can be applied to any structural typology.

Specifically, the idea is to study the fire-performance of the structural system that is damaged due to seismic actions, scaling the earthquake intensity, in order to represent more severe earthquake with lower probability of occurrence; thus causing different levels of damage in the structural system. The target is to evaluate the reduction of the fire-resistance of the structure due to the earthquake induced damage. The reduction is referred with respect to the case where the structure is not damaged. In the latter case, the fire resistance is indicated as the reference one in this study. The comparison of the results concerning the FAE scenarios with the reference case indicates the reduction of the fire resistance due to the induced damage. The fire-resistance of the structure is calculated using limits based on the ductility of structural members at elevated temperatures. These limits take into account the material deterioration as the temperature increases, the induced damage in the structural members due to prior seismic loading and the effect of geometric initial imperfections.

2. Seismic and Gravity design of the considered building

The building that is considered in this study is a 4-storey steel framed structure used as a library. The plan-view of the building is illustrated in Fig. 1(a). All the levels are similar and the height of the floor is equal to 3.5 m. The library building is initially designed in order to resist the gravity and seismic loading. It is important to notice that this paper is devoted to the case where the structures are "well-designed" according to the guidelines of Eurocode 8 (2004) and Eurocode 3 (2003). In other cases, if the buildings do not conform to the seismic and gravity design rules,

the results would be completely different and for this reason these cases are out of the scope of this paper.

The study is focused on a typical frame oriented in the *y*-direction of the building as it is indicated in Fig. 1(b). The area loads (permanent and live) that are considered, according to Eurocode 1 (2001), for the design of the library building are the following: permanent load $G = 7.6 kN/m^2$ and live load $Q = 3kN/m^2$ for the upper level and $5kN/m^2$ for the rest levels. Initially the frame is designed for the Ultimate Limit State (ULS) combination of actions for the gravity loading. It is noted that a concrete slab of total depth equal to 0.2 m is assumed to be present at each floor of the building. The seismic design of the structure is conducted according to Eurocode 8 (2004). The design effect of actions for the seismic design can be obtained using the combination for accidental situation. The combination is simplified to the expression $G + \psi_2 Q \pm E$. The value of the coefficient ψ_2 that is applied to the variable action Q is considered to be equal to 0.8 according to Eurocode (2006).

Specifically, the frame is designed to withstand the design seismic action without local or global collapse, thus retaining the structural integrity and a residual load bearing capacity after the seismic events. The previous, according to the guidelines of Eurocode 8 (2004), define that the frame is designed to meet the ULS (or "no-collapse") requirements.

(a)

(b)   (c)
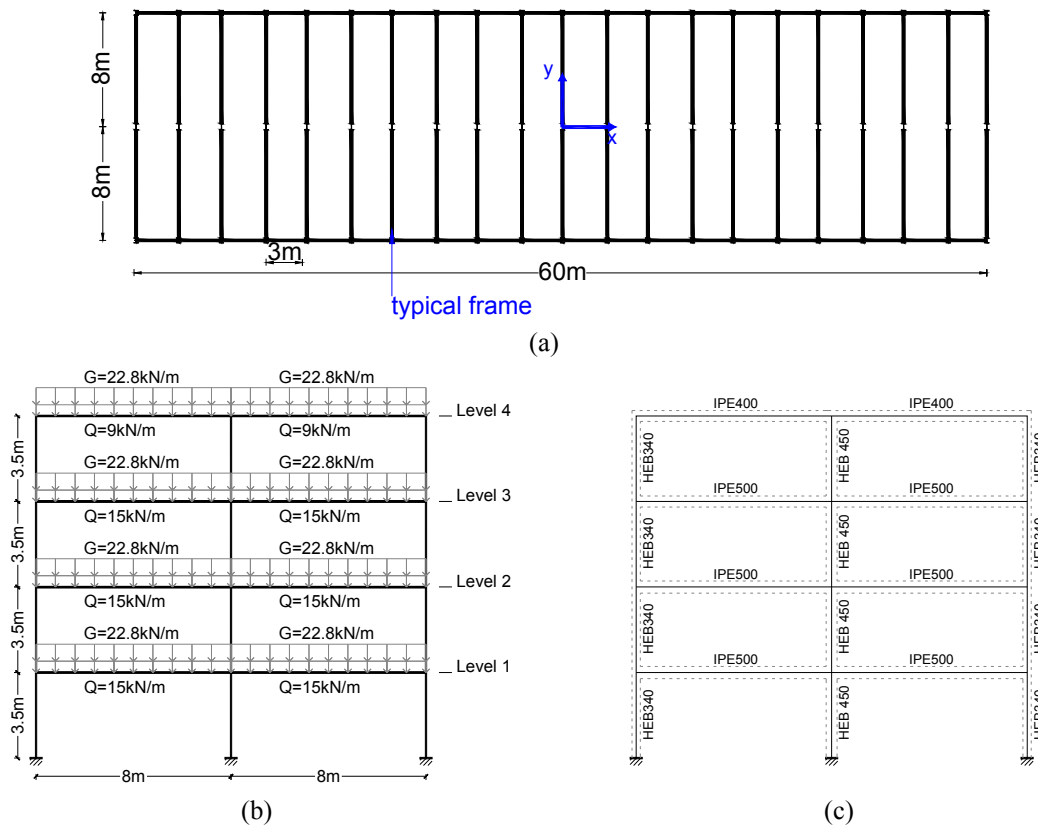
Fig. 1 (a) The structural system- plan-view, b) Typical frame c) The cross-sections of the typical frame according to the design for seismic and gravity loading

For the needs of this study, the seismic action is represented through the elastic response spectrum $S_e(T)$ of Type 1. The soil type is considered to lie in the D category. The design ground acceleration α_g is taken equal to 0.36 g. The design spectrum ($S_d(T)$) that is used in this study is based on the elastic one taking into account that the behaviour factor q is equal to 4. The value of the behaviour factor is selected according to the specific rules for steel buildings and indicates that the frame is designed according to the concept of dissipative behaviour. Specifically, according to Tables 6.1 and 6.2 of Eurocode 8 (2004) this behaviour factor corresponds to the medium ductility class and to regular buildings that are formed using moment resisting frames. In order to verify the design requirements, the lateral force method of analysis is used.

The global and local ductility condition is verified in order to ensure that both the structural members and the structure as a whole, possess adequate ductility. The calculations verify that the soft storey plastic mechanism is prevented. Moreover, the capacity design rules are verified according to general requirements included in Section 4.2.3 of Eurocode 8 (2004) and the specific rules for steel buildings that are given in Section 6.6 of Eurocode 8 (2004). Since the capacity design rules are satisfied, it is ensured that regarding the plastic hinges, the full plastic moment resistance and the rotational capacity are not decreased by compression and shear forces. Additionally, the capacity design indicates that the plastic hinges are formed at the beams ends but not in the columns. This is only violated at the base of the moment resisting frame. The cross-sections of the structural members that result according to the design procedure are summarized in Fig. 1(c).

3. Numerical modelling

The two-dimensional model for the simulation of the behaviour of the steel frame is developed through the non-linear finite element code MSC-Marc (2011) and uses the element of type 98 of the library of the software. The cross-section of the finite element is a user-defined solid numerically integrated one. Four different branches are assigned for the simulation of the sections of structural members: the upper flange, the web (which is divided into two parts for more accurate results) and the lower flange branch. For every branch 25 different integration points are defined. The stress-strain law is integrated using the Newton-Cotes rule. The results are exported for the different integration points. In total 595 finite elements are used for the numerical simulation The discretization is not uniform in order to decrease the total number of the finite elements that are used in the simulation and consequently the computational time that is required for the analysis. Regarding the beams, the mesh is more dense at the support position and at the mid-span, in order to capture their nonlinear behaviour. It is noted that the beam-column joints details are not included in the numerical model. For this reason, rigid offsets are used in order to model the connections between the beams and the columns. This indicates that the joint are assumed to be rigid.

The yield stress of the structural steel is assumed to be equal to 275MPa at room temperature. It is noted that the strain hardening of steel for the temperature range of 20°C-400°C is neglected in order to simplify the problem.

Initially, two different models are developed. In the first model all the finite elements are using the elastic-perfect plastic material law (distributed plasticity model - DPM) while the second model is based on the concentrated plasticity approach i.e., the elastic-plastic behaviour of the model is consolidated at the ends of beams and columns and at the mid-span of beams. The rest of

Table 1 The time-history acceleration records used for dynamic analyses

Waveform ID	Earth. Name	Mw	Fault Mechanism	Duration (sec)	Epicentral Distance [km]	EC8 Site class	PGA [m/s^2]	S.F.
290xa	Campano Lucano	6.9	normal	71.93	32	A	2.248	2.121
293ya	Campano Lucano	6.9	normal	83.94	33	B	4.890	0.975
6142ya	Aigion	6.5	normal	39.5	43	B	5.235	0.911
612xa	Umbria Marche	6	normal	106.21	38	B	5.316	0.897
1726xa	Adana	6.3	strike slip	29.2	30	C	2.210	2.158
1726ya	Adana	6.3	strike slip	29.18	30	C	1.803	2.644
5850xa	Strofades	6.6	oblique	65.43	38	B	3.699	1.289

the finite elements are considered to be elastic. The first model, which simulates accurately the frame behaviour, is developed in order to study carefully the seismic response. The second model, which is based on the assumption of the concentrated plasticity (CPM), is developed in order to simplify the numerical analyses. More specifically, using first the results of the DPM analyses, the seismic behaviour of the frame structure is obtained. Taking into account the previous results, the positions where the plastic hinges are formed are assigned and the CPM is developed. Thus, the elastic-plastic material law is attached at the finite elements that correspond to the plastic hinge locations.

4. Non-linear analysis for seismic excitation

4.1 Representation of seismic actions

Artificial accelerograms are generated in order to represent the seismic action. To this end the Rexel (Iervolino *et al.* 2010) software is used, which is a computer aided record selection tool for code based seismic structural analysis. The time-history acceleration records that result are then properly scaled in order to match the elastic spectrum using the appropriate scale factors. The characteristics of the seven accelerograms that are used in this study are summarized in Table 1.

The problem is solved numerically using the Finite Element Method (FEM) through dynamic transient analysis with direct integration of the equations of motion and the "large strain formulation" is used.

The selection of the numerical procedure used for the time integration of the differential equations is crucial. The three most important aspects are: the convergence of the solution, the stability and the accuracy. In this study the Newmark-Beta method, as implemented in MSC MARC (2011), is used applying the linear acceleration scheme ($\gamma = 0.5$ and $\beta = 0.25$). The time-step of the analysis is set to be constant and equal to 10^{-3} sec.

4.2 Incremental Dynamic Analysis (IDA)

Table 2 Scaling of the seismic action

Scale Factor (S.F.)	1.25	1.50	1.75	2.00
PGA	0.608g m/sec^2	0.729g m/sec^2	0.851g m/sec^2	0.972g m/sec^2

Lower probability of existence –More severe earthquakes

The next step of the study is the evaluation of the earthquake response of the structure through Incremental Dynamic Analysis (IDA). IDA is a parametric analysis method for the estimation of the structural performance under seismic loads (Vamvatsikos and Cornell 2002). Specifically, the structure is subjected to one (or more) ground motion records, each scaled to multiple levels of intensity. In this way the behaviour of the structure can be represented through response curves parameterized versus the intensity level. Initially, two issues must be addressed in order to proceed to the IDA analysis. The first one is the definition of the quantity that characterizes the intensity of the ground motion. The second is to determine a response quantity for the classification of the structural behaviour. In this study the intensity of the ground motion record is represented through the PGA. On the other hand the response of the structural system is represented through both the base shear and the maximum drift angle.

The seven accelerograms are scaled with respect to the PGA using the scale factors (S.F.) that are defined in Table 2. It is noted that as the scale factor increases the time-history acceleration records represent more severe ground motions and the return period is higher.

4.2 Results of IDA - Verification of performance levels

The results of the IDA are presented in terms of inter-storey drift angle versus PGA. Actually, two different IDA curves are obtained for a single accelerogram. The first one uses the maximum recorded (transient) inter-storey drift angle while the second corresponds to the residual drifts (Fig. 2(a), Fig. 2(b) and Fig. 2(c)). At this point, the response of the structural system is verified with respect to the limit values for the drift angles that are recommended in FEMA 356. Specifically, the limit values for the drift angles of steel moment frames that correspond to three different performance levels are adopted. For the Collapse Prevention (C.P.) performance level the limit
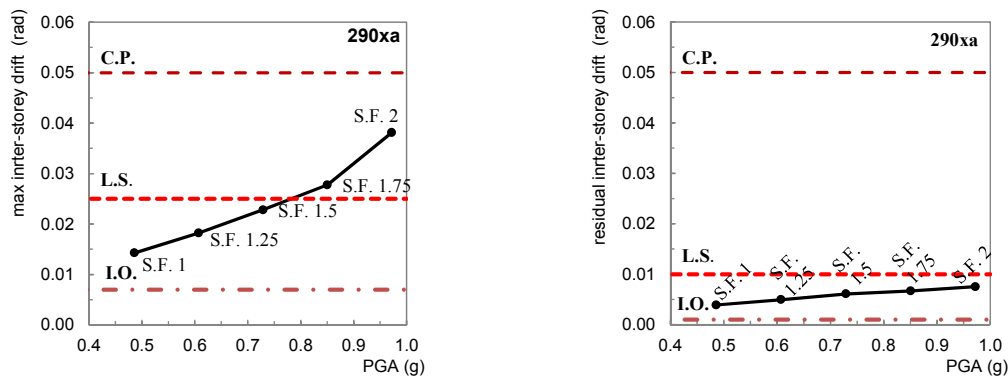
Fig. 2(a) IDA curves in terms of maximum inter-storey drift angle and PGA. (accelerograms 290xa)

value for permanent or transient drift is defined to be equal to 5%. In the case of the Life Safety (L.S.) performance level the limit values are 2.5% for the transient drift and 1% for the permanent one.

Finally, more severe limits are used in the Immediate Occupancy (I.O.) performance level where it is recommended that the transient drift angles should not exceed the limit of 0.7% and the residual angles should be negligible. In order to quantify the term negligible the limit value is set equal to 0.1%. The structural performance limits are depicted in the diagrams of Fig. 2. It is concluded that according to the specific limits for the transient drift, the structural response lies
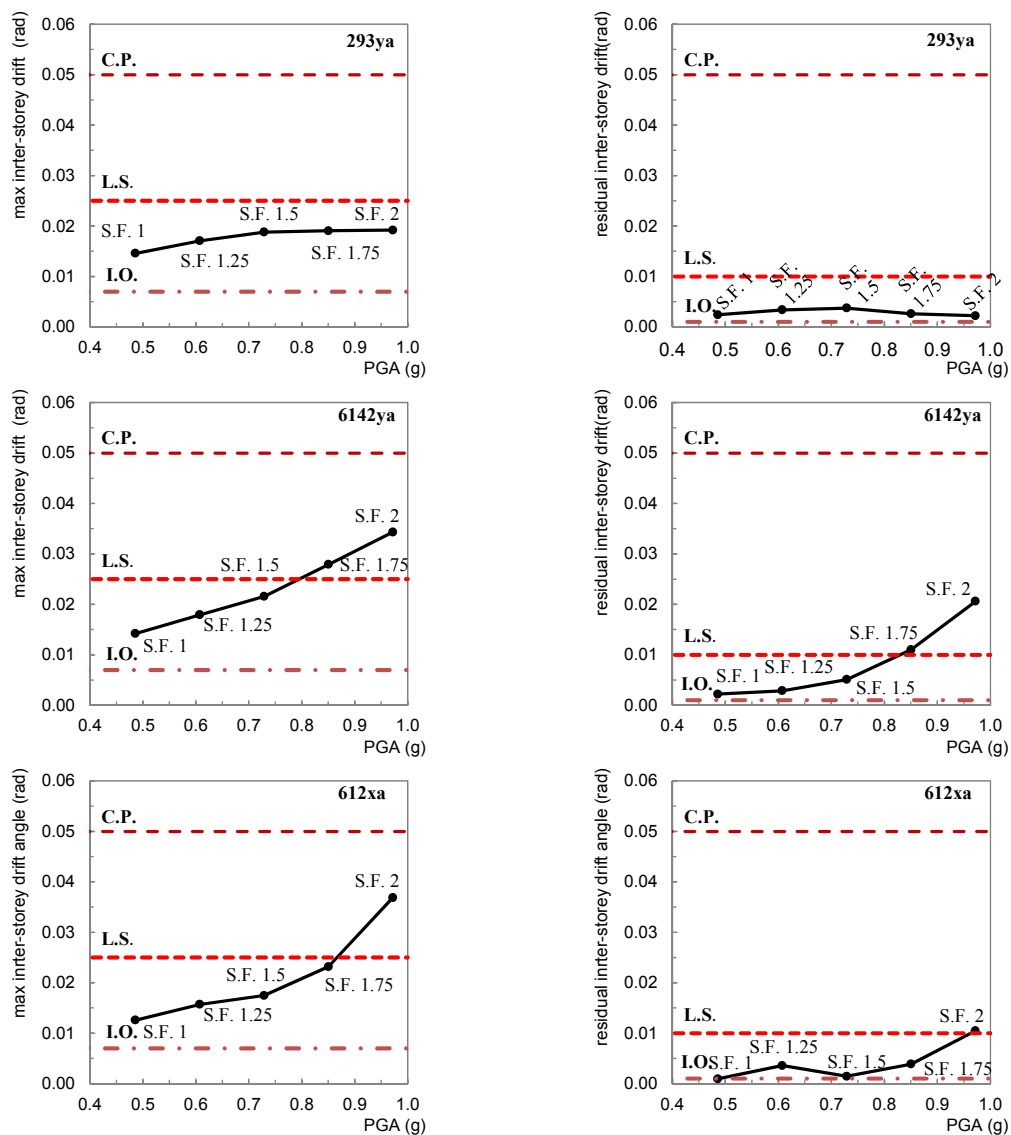
Fig. 2(b) IDA curves in terms of maximum inter-storey drift angle and PGA. (accelerograms 293ya, 6142ya and 612xa)

Daphne Pantousa and Euripidis Mistakidis
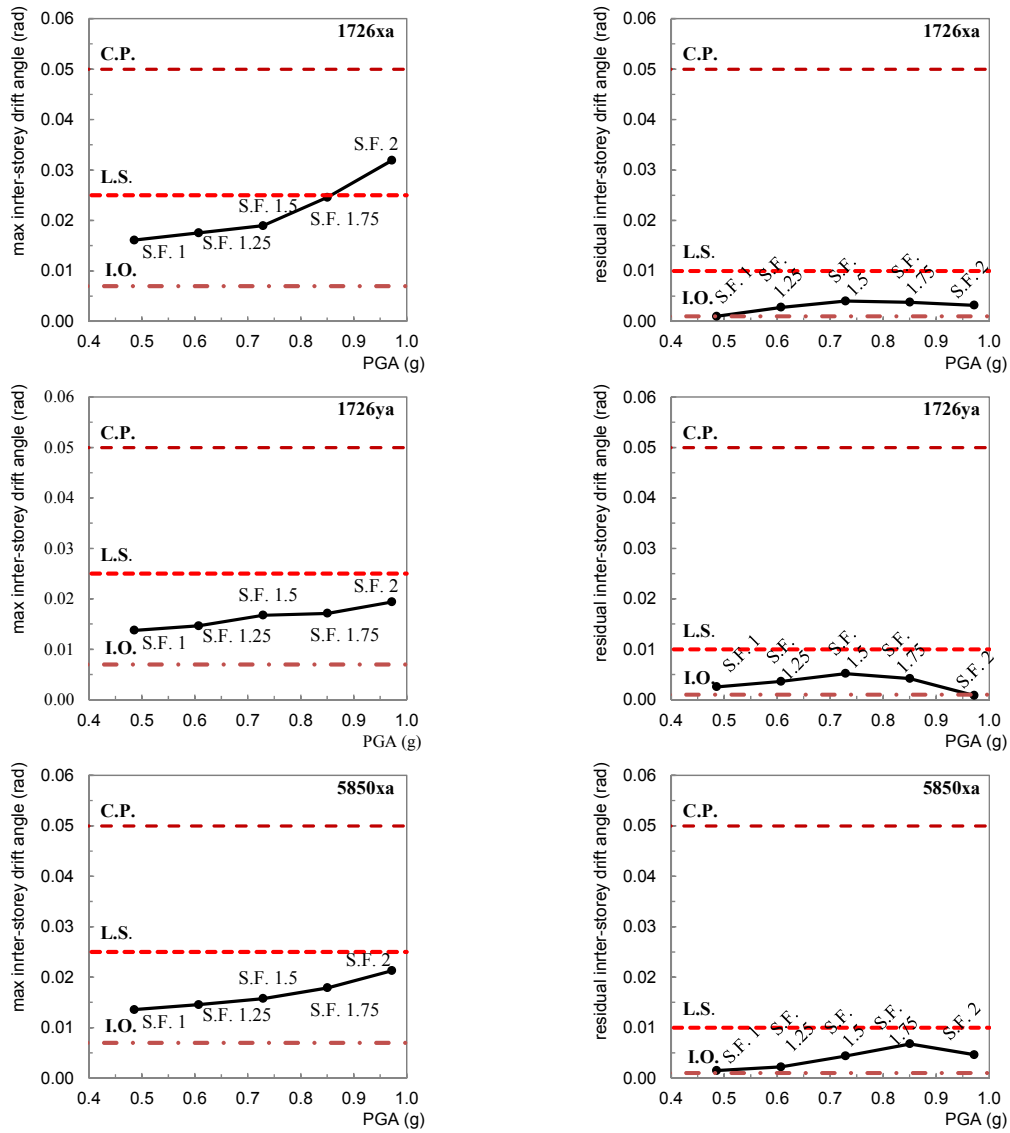
Fig. 2(c) IDA curves in terms of maximum inter-storey drift angle and PGA. (accelerograms 1726xa, 1726ya and 5850xa)

between the I.O. and the L.S. performance levels when the S.F. is bounded in the interval 1.00 to 1.75. This is valid for all the accelerograms that are studied, with the exception of the cases 290xa and 6142ya. In these specific cases the structural response for S.F. equal to 1.75 is allocated between the L.S. and the C.P. states. Taking into account the permanent drift angles, the response of the structure is limited between the I.O. and the L.S. limits. It is noted that for S.F.>1.75 the results of the analyses, considering the deflection and the strain field, are not realistic. For this reason the case of S.F.=2 is not further studied.

5. Characterization of the seismic damage in correlation with the seismic loading level

The next goal is to define the 'level of damage' that is induced to the structural system due to the earthquake excitation. Various damage indices are proposed in the literature (Cosenza and Manfredi 2000, Kappos 1997). The damage measures for the non-linear structural response are defined either for individual structural elements (local indices) or they are related to the entire global structure (global indices) and they are used in order to define the damage potential in global or local level. The approaches that are proposed are based mainly in terms of plastic dissipated energy and on the ductility of the structural systems. In this study a simplified approach is obtained. Specifically, in order to focus to individual structural members, the *maximum plastic strain* at the plastic hinge locations, at the end of the seismic excitation is used in order to simulate the 'level of damage'. It is clear that the *maximum plastic strain* depends on the plastic hinge mechanism allocation at the end of the earthquake, the time-history acceleration record and the intensity of the earthquake. It is noted that the *maximum plastic strain* that is used here intends only to the characterization of the damage of the structural components at the end of the earthquake and it is further used in order to determine the fire resistance of the structural system through rotational limits (Section 9).

Table 3 *Maximum plastic strain* at the ends of the beams of the first level

Accelerogram/Beam		S.F. 1.00		S.F. 1.25		S.F. 1.50		S.F. 1.75	
		L	R	L	R	L	R	L	R
290xa	Beam 1A	0.020	0.020	0.045	**0.082**	0.099	**0.138**	0.181	0.221
	Beam 1B	0.020	**0.035**	0.050	0.077	0.105	0.131	**0.319**	0.210
293ya	Beam 1A	**0.044**	0.035	0.077	0.077	0.123	**0.133**	0.187	**0.203**
	Beam 1B	0.044	0.032	**0.079**	0.067	0.125	0.117	0.191	0.181
6142ya	Beam 1A	0.081	**0.089**	0.146	0.139	0.220	0.222	0.305	**0.329**
	Beam 1B	0.080	0.081	**0.151**	0.126	**0.227**	0.203	0.315	0.306
612xa	Beam 1A	**0.032**	0.028	0.093	0.083	0.207	0.203	0.347	**0.361**
	Beam 1B	0.032	0.023	**0.096**	0.073	**0.213**	0.190	0.353	0.341
1726xa	Beam 1A	0.046	0.046	0.088	**0.102**	0.158	0.162	0.218	0.209
	Beam 1B	**0.047**	0.043	0.086	0.098	0.158	0.152	0.222	0.197
1726ya	Beam 1A	**0.033**	0.022	0.059	0.058	0.087	**0.105**	0.116	**0.148**
	Beam 1B	0.033	0.020	**0.059**	0.055	0.089	0.096	0.119	0.135
5850xa	Beam 1A	0.016	**0.022**	0.037	**0.041**	**0.070**	0.058	0.111	0.097
	Beam 1B	0.014	0.021	0.034	0.037	0.070	0.050	**0.118**	0.079
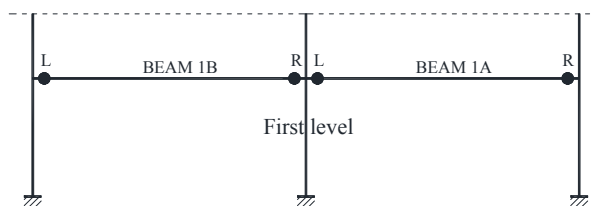
Fig. 3 Identification of the ends of the beams that are presented in Table 3

In the sequel, the study focuses on the structural members of the first level of the structural system where the fire exposure is assumed to take place. Table 3 presents the *maximum plastic strain* values for the scaled-up time-history acceleration records that are used in this study. The maximum plastic strain values are calculated for both ends (**L**eft and **R**ight) of each beam (Beam 1A and Beams 1B) as it is illustrated in Fig. 3.

6. Non-linear structural analysis for fire loading

6.1 Representation of fire loading - Numerical modelling

In this Section the behaviour of the structural system for the *reference* fire scenario is studied. As it is already mentioned, the fire is assumed to take place in the first floor of the library building. The *reference* scenario is determined using the ISO fire curve (SC-ISO). The first objective is to calculate the temperature profiles of the structural members. To this end, the temperature in the fire-compartment is assumed to be uniform. The temperature profile of the structural members is presented in Fig. 4. It should be emphasized that no thermal analysis is conducted and the temperature profile for the structural members is calculated according to the guidelines of Eurocode 1 (2001), depending on the cross-section dimensions. Moreover, it is assumed that the temperature is uniform along the member and the thermal gradient in the cross-section is not taken into account.

It is highlighted that, regarding the reference scenario, the structure is considered to be undamaged and thus the results of the analysis specify the inherent fire-resistance of the structural system. During the fire exposure, the loading combination of permanent and live actions according to the guidelines of Eurocode 3 (2003) is taken into account. Since the fire is classified as an accidental action (Eurocode 2006), the design effect of actions for the fire situation can be obtained using the combination for accidental situation. The combination is simplified to the expression $G + \psi_2 Q$. The value of the coefficient ψ_2 that is applied to the variable action Q is considered to be equal to 0.8, according to the guidelines of Eurocode (2006) for library buildings.
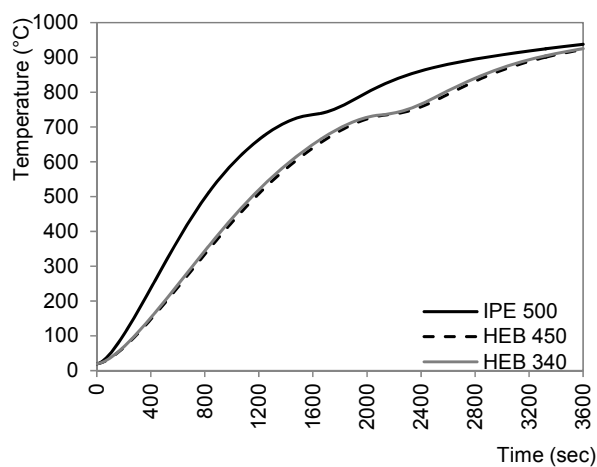
Fig. 4 Temperature profile of the structural members for the ISO *reference* scenario

The numerical model that is developed for the simulation of the fire behaviour of the structural system is the same with the one already presented. The model uses beam finite elements and the material properties (mechanical and thermal) are taken according to the guidelines of Eurocode 3 (2003). The problem is solved through non-linear dynamic analysis as it is described in the previous section.

6.2 Results of numerical analyses for the SC-ISO

The deformed shape of the structural system at the end of the numerical analysis is illustrated in Fig. 5. The analysis stops at the 1584th sec (26.4 min) due to convergence failure. The same figure presents the distribution of the maximum plastic strain along the beam. It is concluded that the structural system fails due to the formation of a local unstable mechanism at the heated beams.

In order to understand thoroughly the fire response of the heated beams, the evolution of Von Mises stress with temperature for the Nodes 2437 (Left end), 2439 (Right end) and 3240(Mid-span) are presented in Fig. 6. The stresses are studied for both the Upper Flange (UF) and the Bottom Flange (BF). All the figures include the reduction of both the yield and the proportionality limit stresses (according to EN1993-1-2) as the temperature increases. It is observed that the stress of the BF at the left support reaches the proportionality limit value (point A) for a temperature approximately equal to 320°C (520th sec). This indicates that plastic strains appear in the cross-section. Next, the proportionality limit is attained at the compression flange at the mid-span (point B) for a temperature equal to 380°C (610thsec). The stress at the UF at the left support becomes equal to the proportionality limit (point C, 475°C, 765th sec) and the same happens very quickly
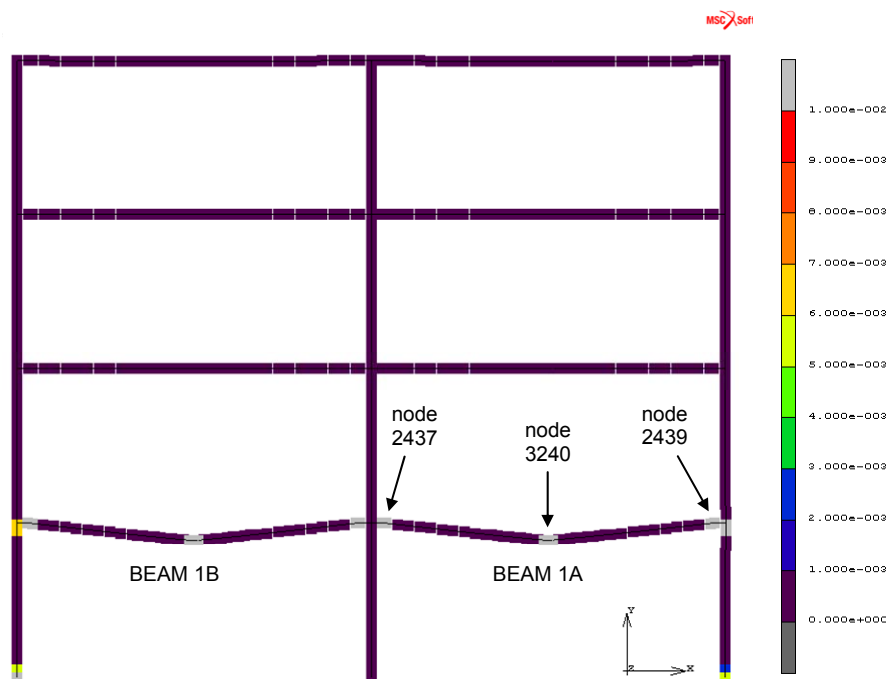
Fig. 5 Deformed configuration of the structural sub-system at the end of analysis

(a)

(b)

(c)
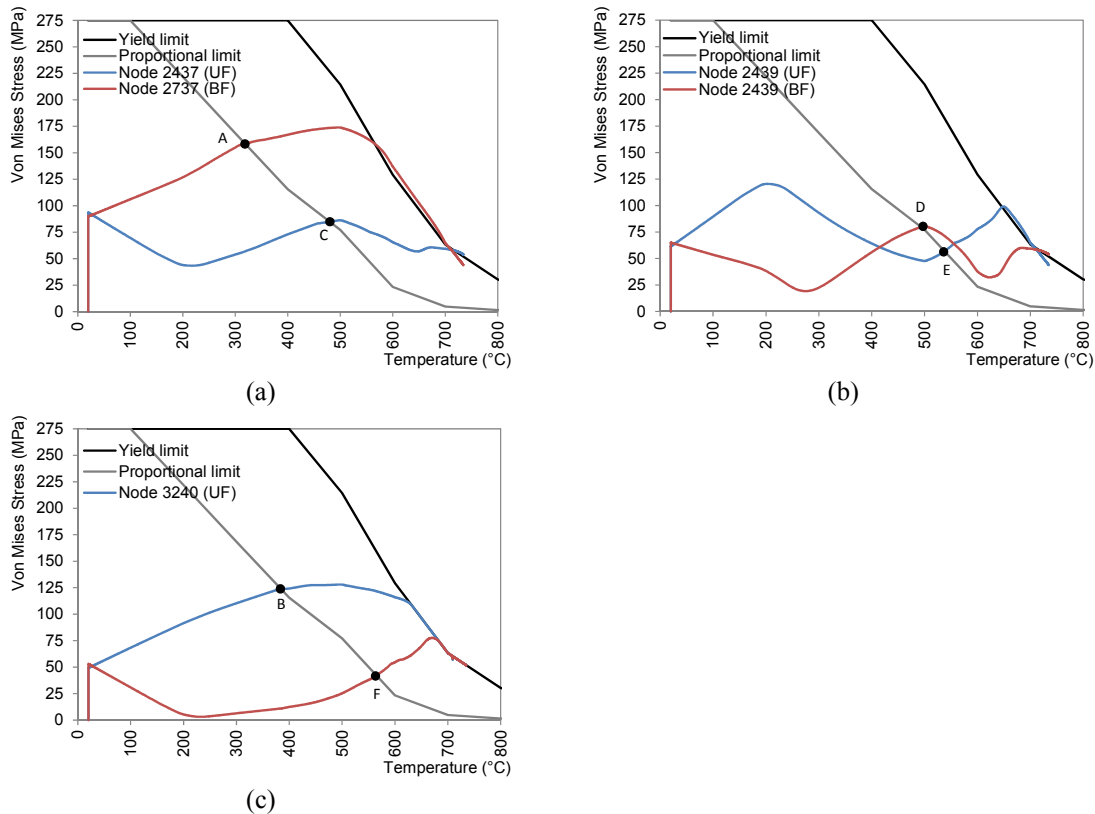
Fig. 6 Von Mises stress evolution with temperature at the upper and the lower flange (a) in the left end, (b) in the right end and (c) in the mid-span of Beam 1A

for both the bottom and the upper flange of the right support (points D and E, 490 and 540°C, 790th and 880th sec respectively). Finally, it is interesting to notice that the Von Mises stress time-evolution is completely different at the left and the right ends of the beam. This is attributed to the different rotational and axial restrains that are provided by the adjacent members at the respective positions.

7. Non-linear analysis for fire-after earthquake loading

7.1 Fire-after-Earthquake scenarios - Numerical modelling

The seismic action is simulated through the time-history acceleration records that were presented in previous Sections. On the other hand, the fire action is simulated through the ISO-fire curve. The temperature time-history curves for the structural members are obtained according to the procedure that is proposed in Eurocode 3 (2003). Actually, the temperature profile is dependent on the geometric cross-section characteristics (see Fig. 4).

The numerical model used for the simulation of the behavior of the structural system during the Fire-After-Earthquake loading is identical with the one that was described in Section 3. Moreover,

Table 4 ISO-FAE scenarios

		Time-history acceleration record						
		290xa	293ya	6142ya	612xa	1726xa	1726ya	5850xa
Scale factor	1.00	E290xa/1.00-FISO	E293ya/1.00-FISO	E6142ya/1.00-FISO	E612xa/1.00-FISO	E1726xa/1.00-FISO	E1726ya/1.00-FISO	E5850xa/1.00-FISO
	1.25	E290xa/1.25-FISO	E293ya/1.25-FISO	E6142ya/1.25-FISO	E612xa/1.25-FISO	E1726xa/1.25-FISO	E1726ya/1.25-FISO	E5850xa/1.25-FISO
	1.50	E290xa/1.50-FISO	E293ya/1.50-FISO	E6142ya/1.50-FISO	E612xa/1.50-FISO	E1726xa/1.50-FISO	E1726ya/1.50-FISO	E5850xa/1.50-FISO
	1.75	E290xa/1.75-FISO	E293ya/1.75-FISO	E6142ya/1.75-FISO	E612xa/1.75-FISO	E1726xa/1.75-FISO	E1726ya/1.75-FISO	E5850xa/1.75-FISO

the problem is solved through dynamic analysis based on the direct integration of the equations of motion as it was described in Section 4. All the details concerning the type of the numerical analysis are identical.

Here, the difference lies to the fact that the numerical analysis consists of two different stages. In the first stage the structural system is submitted to the seismic action until the oscillation is totally damped. In the second stage the structural members of the first level of the frame structure are exposed to fire. The ISO-FAE scenarios are displayed in Table 4. Four FAE-scenarios are defined for one accelerogram according to the scaling factors that are used for the intensity of the earthquake action. Thus, totally 4×7=28 ISO-FAE scenarios are generated.

7.2 Results for the Fire-After-Earthquake scenarios

The results of the numerical analyses indicate the failure mechanism of the structural system under the FAE scenarios. In all the cases that are studied, the same failure mechanism evolved (local unstable mechanism at both beams that were exposed to fire) as the one that is observed in the *reference* fire scenario.

In general, it is concluded that numerical analysis stops due to convergence failure which is a result of the unstable kinematic mechanism that is developed. Fig. 7 presents the evolution of the mid-span deflection of Beam 1A with time for all the ISO-FAE scenarios. Each diagram corresponds to a specific ground motion acceleration record. As the scale factor used for the amplification of the earthquake intensity increases, the mid-span deflection curve is shifted accordingly. This holds for all the cases that are considered in this study.

The next objective is the calculation of the fire resistance of the structural system (in time or temperature domain). Obviously, the fire resistance time does not coincide with the numerical analysis time since the analyses stops due to numerical convergence. On the other hand, the deflection criteria that are usually used in practice are not appropriate in the present case, since they tend only to limit the extensive deflections that take place during the fire-tests. If these criteria are used there is no obvious difference between the distinct cases studies, since the limit values of deflection take place almost at the same time for all the cases. Thus, it is essential to define alternative limits for the definition of the fire-resistance of the structural system. The limits should take into account the deterioration of the mechanical properties at elevated temperatures and, moreover, in the case of the structures that are damaged due to earthquake, the limits should be modified depending on the 'level of prior seismic damage'. In this study rotation limit values are utilized as it is demonstrated in the next Section.
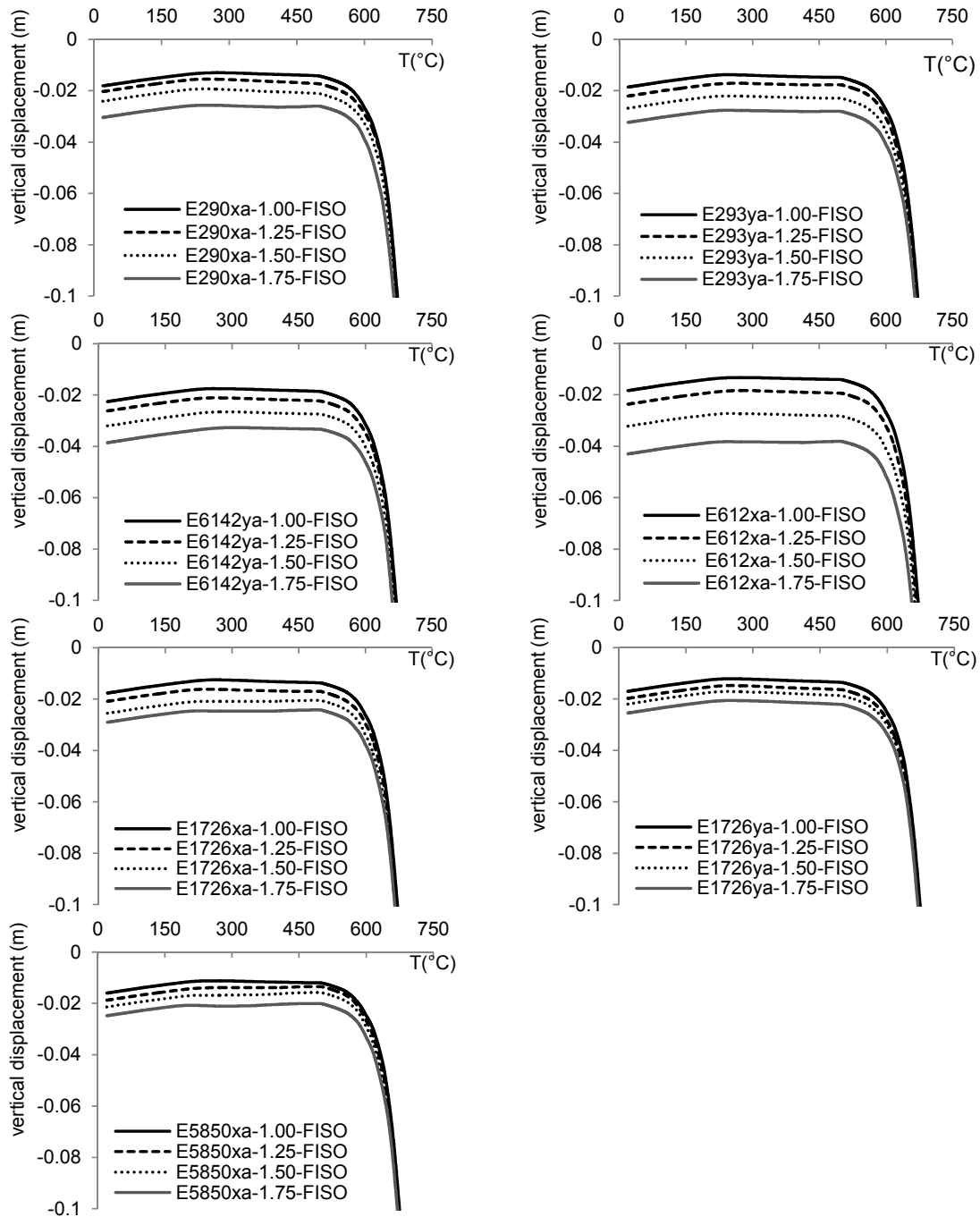
Fig. 7 Vertical displacement at the mid-span of Beam 1A versus temperature

8. Failure of the structural system at elevated temperatures

Next, the study is focused on the identification of the failure conditions of the structural system

under fire and FAE loading. As it was concluded in the previous Section, the numerical analysis stops due to the formulation of an unstable kinematic mechanism at the heated beams and large deflections arise. Instead of using deflection criteria, an alternative way is to consider the moment-rotation behavior at the plastic hinge locations i.e., at the ends of structural members. In this study it is considered that the fire-resistance time is the time where the rotational capacity of a structural member is exhausted. Therefore the fire resistance of the structural system is calculated using the ultimate values of plastic rotation of structural members at elevated temperatures as it is presented in detail in the study of Pantousa and Mistakidis (2014). These values are used in order calculate the fire-resistance time and do not indicate the final collapse of the structural system.

The study of Pantousa and Mistakidis (2014) was focused on the calculation of the rotational capacity of steel beams at elevated temperatures. Moreover, limit rotation values for the determination of the fire-resistance of steel structural members under FAE loading were obtained. To this end, three-dimensional shell finite element models were used for the simulation of the behaviour of I-beams at elevated temperatures. The models took into account initial geometric imperfections. First, the models were validated against published experimental results. The problem was solved numerically using non-linear finite element analysis. The analysis had two different stages: the first stage of the cyclic loading (at ambient temperature) and the second stage of the monotonic loading (under constant temperature). Cyclic loading was used in order to simulate the damage that is induced at the ends of the beam (that is actually a member of frame structure) due to earthquake loading. Different cyclic loading patterns (taking into account the level of the imposed displacement) were introduced in order to induce a specified 'level of damage' in the beam. Actually, the ductility of the beams was obtained through virtual three-point bending tests (monotonic loading) under constant temperature, which followed the cyclic loading stage. The study started with the reference case where the beam is undamaged.

Parametric analyses were conducted with respect to the level of the temperature during the monotonic stage and the amplitude of the initial imperfections. In this way, the behavior of the pre-damaged beams was obtained for different temperature levels. Specifically, first the moment-rotation curves were calculated for the monotonic stage of loading and the rotational capacity of the pre-damaged beams at elevated temperatures was obtained. The term *ultimate available rotation* was used to identify the limit rotation value that corresponds to the exhaustion of the available rotational capacity of the beam and can be utilized for the calculation of the fire resistance of steel beams at elevated temperatures. It was concluded that, clearly, the *ultimate available rotation* is not strongly temperature dependent. Moreover, it depends on the amplitude of the initial imperfections and on the amplitude of the imposed displacement during the cyclic loading. Specifically, it was found that the level of the induced damage during the cyclic loading, affects strongly the ultimate available rotation. The aforementioned rotation is considerably reduced when the amplitude of the imposed displacement is escalated and this becomes more important as the amplitude of the initial imperfections increases.

Taking into account the previous, it can be concluded that the *ultimate available rotation* values that correspond to the reference case where the beam is undamaged, can be used for the determination of the fire-resistance of the frame structure that is not damaged due to earthquake i.e., in the case of the *reference* fire scenario. The *ultimate available rotation* values that are obtained using the pre-damaged beams can be utilized for the evaluation of the fire-resistance of the damaged frame structures i.e. for the FAE scenarios. In the next Section the damage that is induced during the cyclic loading stage is defined and the *ultimate available rotation* values are presented in detail in Section 8.2.

8.1 Definition of the 'level of damage' concerning the rotational limits

The values of the *ultimate available rotation*, which are defined through the standard beam approach using detailed three-dimensional (shell) models(see Pantousa and Mistakidis 2014), should be categorized according to the 'level of damage' that is induced in the beam during cyclic loading, in order to be utilized for the evaluation of fire-resistance of the frame structure for the FAE loading. It is reminded that in the latter case (frame structure) *beam* finite element models are used. It is clear that two different types of finite elements are used and that the results of the different analyses cannot be compared directly. The comparison would be confusing since the formulation of beam elements uses assumptions that are not present in the shell formulation. In this point of view, a "common *reference* point" must be specified in order to link the results.

The issue that arises at this point is the *interpretation* of the 'level of damage', which is induced in the standard beam (shell finite element analyses) due to cyclic loading, in terms that are comparable to the 'level of damage' in the frame structure, where the beam finite element formulation is used. As it has already been explained in Section 5, the damage induced in the frame, during seismic loading, is characterized by the maximum recorded value of the plastic strain at the end of the seismic excitation. Actually, the difficulty lies on the fact that the results from the shell finite element analysis indicate the plastic strain distribution in the beam which is not directly comparable with the plastic strain filed as it results from the beam finite element analysis where the concentrated plasticity assumption is used. In order to overcome this issue, the standard beam is *re-simulated*, using beam finite elements (the concentrated plasticity assumption is taken into account), and it is submitted to the same cyclic loading patterns (actually, the cyclic loading patterns used for in the case of pre-damaged beams). In this way, the 'level of damage' for the standard beam is obtained at the end of the cyclic loading and is the *maximum plastic strain* (plastic strain in upper/lower fibers of the cross-section) in the mid-span. The same index is derived from the analysis of the frame structure at the end of the seismic loading (Table 3), since the same type of finite element is used and, moreover, the concentrated plasticity assumption is used in both cases.

Taking into account the previous, the technique which is illustrated in Fig. 8 is followed in this study. The simulation of three-point bending test of the standard beam, at elevated temperatures, is conducted using the "shell" finite element model (step 1a) and the moment-rotation curves are obtained at different temperature levels (step 2a). In the same time, the numerical simulation of the cyclic loading stage for the standard beam is conducted (step 1b), using the beam finite element model, and the same cyclic pattern, as in step 1a, is used. In this way the level of *maximum plastic strain* is calculated (step 2b). Finally, the (discrete) function of the ultimate available rotation with temperature (step 3) is obtained (through the moment-rotation curves found in step 2a which corresponds to the *maximum plastic strain* level that is identified in step 2b. The same procedure is repeated for different amplitudes of imposed rotation (or displacement) during the cyclic loading stage.

8.2 Ultimate available rotation

The values of the ultimate rotation that are used in in this study for the determination of the fire resistance of the structure for the FAE loading are presented in Fig. 9. As it was explained in Sections 8.1 and 8.2, the escalated cyclic loading patters that were used in the study of Pantousa and Mistakidis (2014) resulted to increasing levels of *maximum plastic strain* in the cross-section

of the mid-span of the standard beam. Specifically, five cyclic loading patterns were used (amplitude of imposed displacement: 0.02, 0.03, 0.04 and 0.05m) that resulted to the *maximum plastic strain* values that are illustrated in Fig. 9 (*maximum plastic strain*: 0.045, 0.055, 0.07, 0.011 and 0.14 respectively). It is noted that as the temperature rises, the ultimate available rotation is at first reduced and in the sequel it is slightly increased. On the other hand, the maximum plastic strain induced due to cyclic loading affects strongly the ultimate available rotation. Specifically, the aforementioned rotation is considerably reduced when the level of the maximum plastic strain
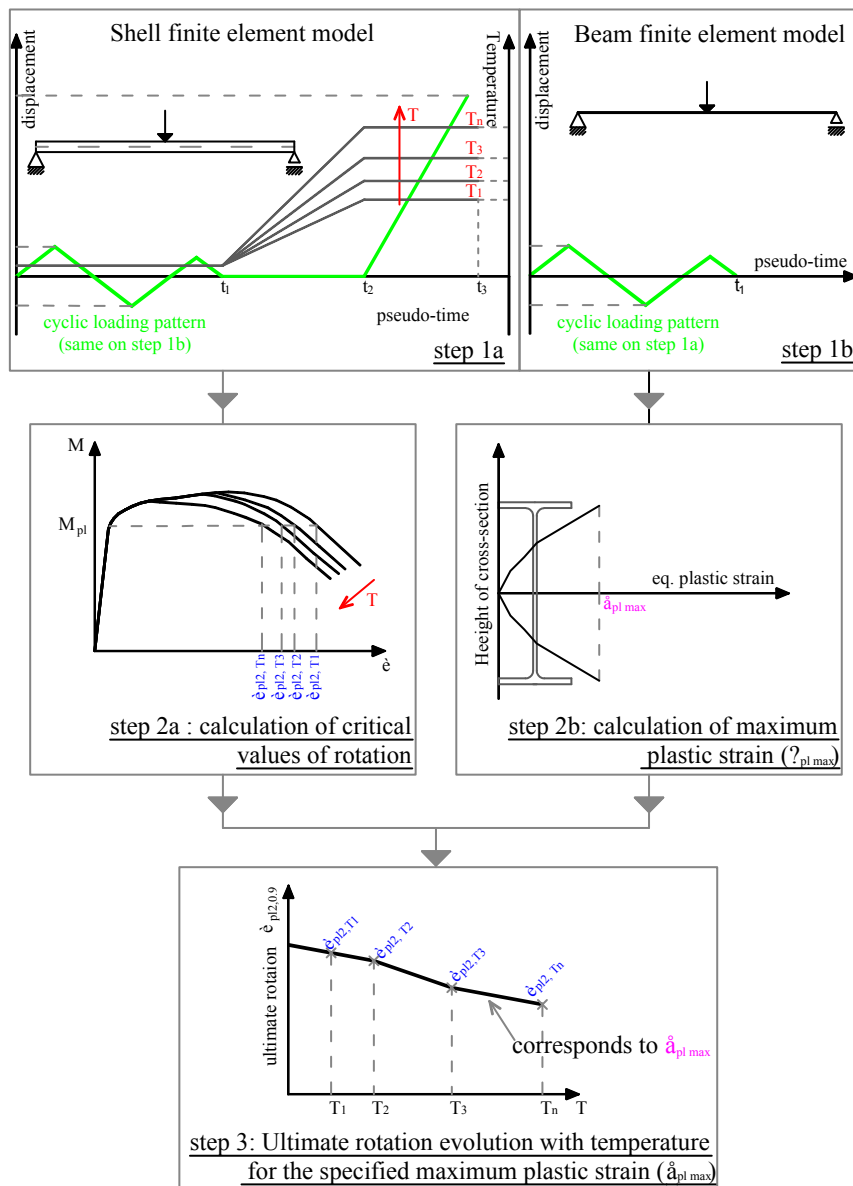
Fig. 8 Proposed procedure for the definition of the *maximum plastic strain*
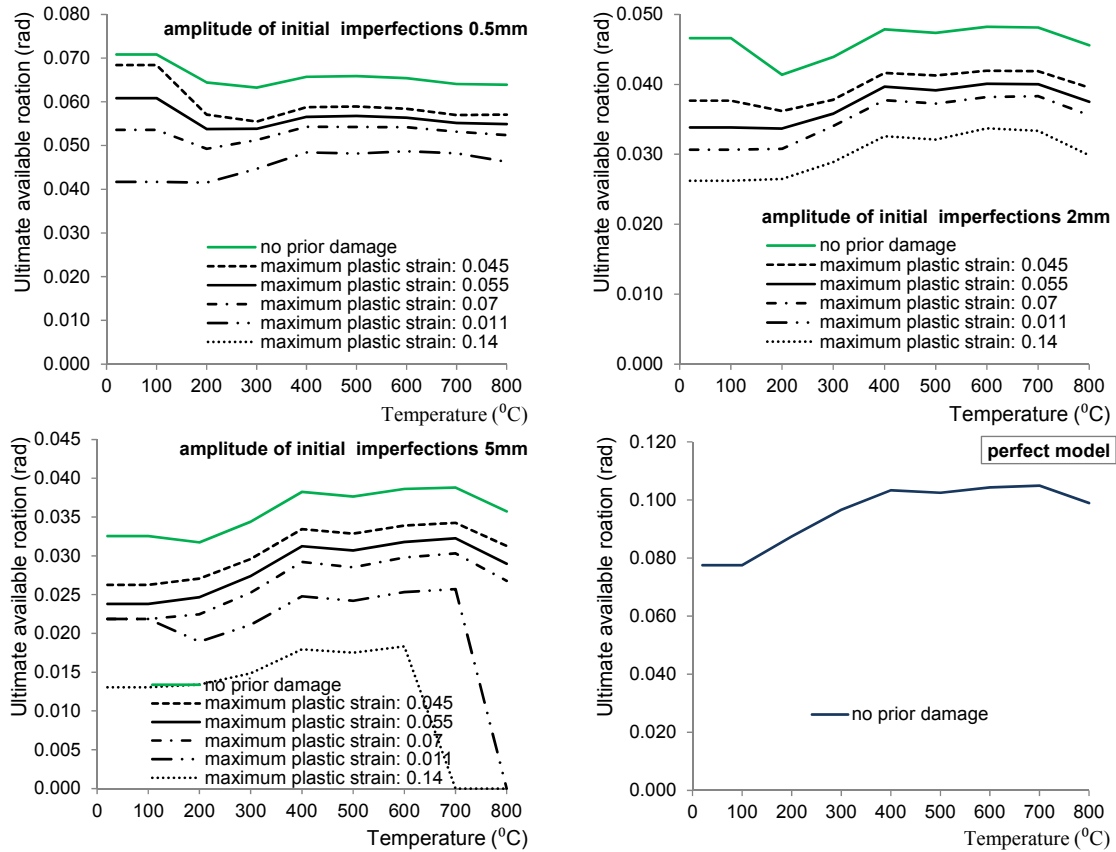
Fig. 9 Ultimate available rotation of the pre-damaged beams for different levels of damage considering the effect of the initial imperfections and for the perfect model

increases and this comes more significant as the amplitude of the initial imperfections increases. Results for the case of the "perfect" model are also given in Fig. 9. In this case the initial imperfections are not considered during the analysis and the ultimate available rotation values are calculated only for the non-damaged beams.

9. Determination of the fire-resistance of the structure for fire and FAE loading

9.1 Determination of the fire-resistance

The behaviour of the heated beams of the frame structure is expressed in terms of rotation (at the support locations) versus temperature since rotational limits are used for the determination of the fire-resistance. In this way, for every heated beam, two different rotation-temperature curves are generated, each one corresponding to each end of the beam. In the case of the *reference* scenario, there is no earthquake induced damage and the corresponding ultimate available rotation values of Fig. 9 should be used. Regarding the cases of FAE scenarios, where the structural system

is damaged due to earthquake, the rotation-temperature curve that corresponds to an individual beam end is characterized by a *maximum plastic strain* value according to Table 3. The ultimate available rotation values that are used for the determination of the fire resistance in this case, must correspond to the same value of *maximum plastic strain*. Linear interpolation is used for intermediate values of *maximum plastic strain* in order to determine the *ultimate available rotation* values of Fig. 9.

The comparison of the rotation of the heated beam of the frame structure with the limit values of the available ultimate rotation of Fig. 9, indicates the *critical value of rotation (θ_{cr})* and the corresponding *critical temperature (T_{cr})*. The critical temperature can be directly connected to the corresponding time of fire exposure (t_{cr}), since the temporal evolution of temperature is already known. In this way the fire-resistance time is calculated. The procedure for the calculation of the fire-resistance in temperature and time domain and the critical rotation value, are illustrated in Fig. 10.

Fig. 10 presents the integrated method for the calculation of the fire resistance of the heated Beam 1A in the case of FAE scenario E6142ya-1.00-FISO. The rotation of the Right and the Left ends of Beam 1A during the fire exposure are plotted in two different diagrams. Each diagram includes the *ultimate available rotation values* of Fig. 9, that are represented though three different curves of the ultimate available rotation as a function of temperature, for amplitude of initial imperfections equal to 0.5 mm, 2 mm and 5 mm respectively. The ultimate available rotation values correspond to a specific *maximum plastic strain level* induced to the end of the beam due to earthquake. In the specific case of Fig. 12, as it is observed in Table 3, the *maximum plastic strain* for the beam at the Left end, is equal to 0.0225 and the corresponding value for the Right end is 0.041.

The intersection of the rotation-temperature curve with the ultimate rotational capacity curve specifies the fire resistance in terms of temperature and the critical rotation value. In this way, for a specific position (Left or Right end), three different intersection points are defined depending on the amplitude of initial imperfections that is taken into account. Then, the fire resistance in time domain is calculated taking into account the time-history temperature of the structural member, according to Fig. 10. Considering specific amplitude of initial imperfections, the critical fire resistance is the minimum value between those corresponding to the Left and the Right ends. For the case that is presented in Fig. 10 the fire resistance (in time and temperature domain) and the critical rotation values are presented in Table 5. The same procedure is repeated for beam 1B. The minimum fire-resistance between the values that correspond to the different heated beams indicates the ultimate limit state where the failure of the structural system is considered to take place.

Table 5 Fire resistance of Beam 1A for the FAE scenario E6142ya-1.00-FISO for different amplitudes of initial imperfections

Amplitude of imperfections		
0.5 mm	2 mm	5 mm
t_{cr}=1336 sec	t_{cr}=1282 sec	t_{cr}=1244 sec
T_{cr}=699.7°C	T_{cr}=686.6°C	T_{cr}=676.5°C
θ_{cr}=0.053rad	θ_{cr}=0.038 rad	θ_{cr}=0.030 rad
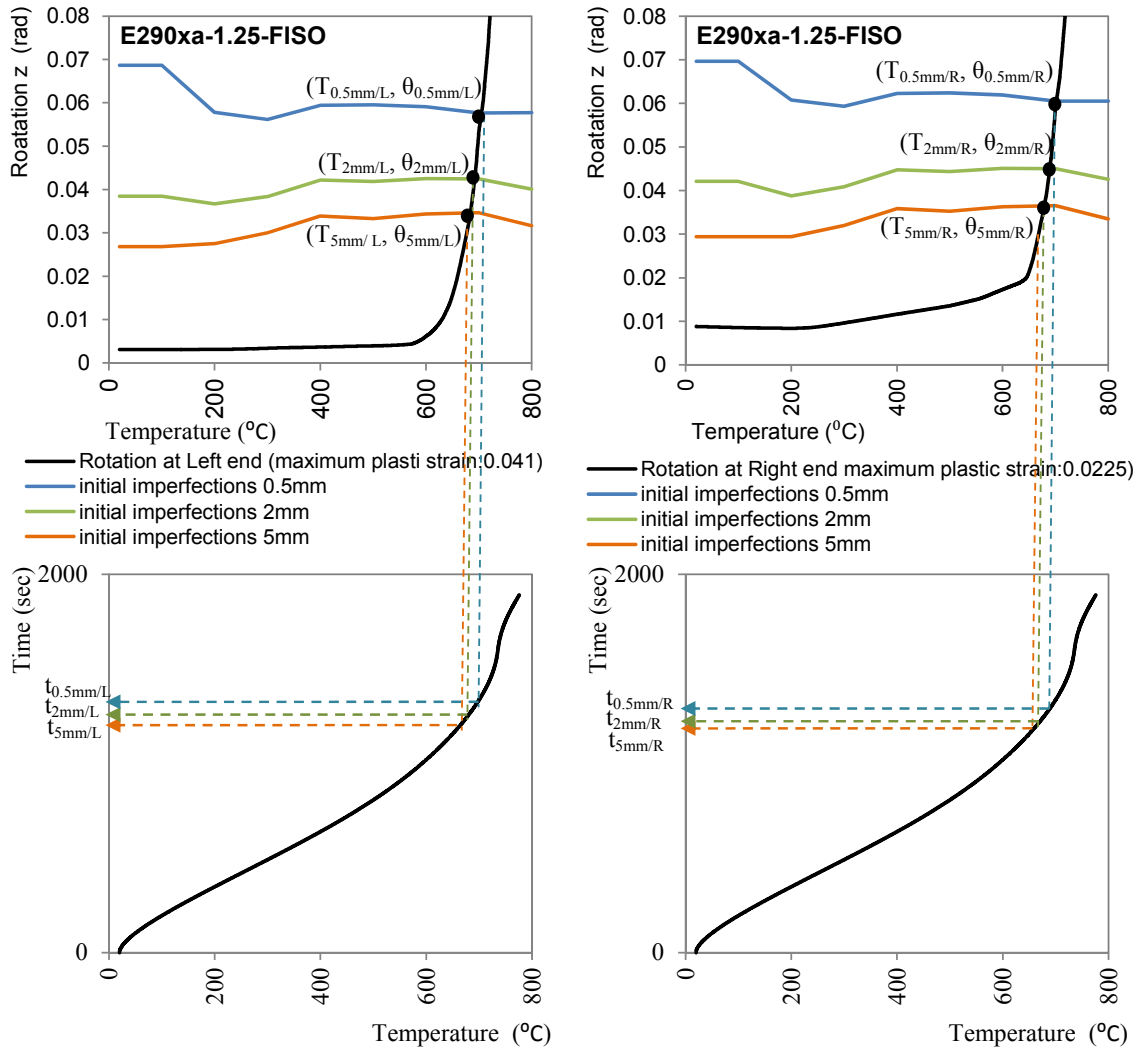
Fig. 10 Calculation of the fire-resistance of heated beams in terms of temperature and time

9.2 Fire-resistance for the reference scenarios

The procedure that was described in the previous section is applied now for the determination of the fire-resistance of the structural system for the *reference* fire scenario. Actually, the fire resistance is calculated taking into account the ultimate available rotation values that correspond to both perfect and imperfect structural members. The results are summarized in Table 6.

9.3 Fire-resistance for the ISO-FAE scenarios

The results are presented, in time domain, in Table 7 for different amplitudes of initial imperfections (0.5 mm, 2 mm and 5 mm). Two different comparisons are conducted. In the first

Table 6 Fire-resistance of the structural system (in terms of time, temperature and rotation)

	No imperfections	Amplitude of initial imperfections		
		0.5 mm	2 mm	5 mm
t_{cr}	1563 sec	1388 sec	1323 sec	1291 sec
T_{cr}	733.3°C	710.7°C	696.7°C	688.9°C
θ_{cr}	0.103 rad	0.064 rad	0.048 rad	0.039 rad

case, the mean value of the fire-resistance time (taking into account the seven different accelerograms) is compared with the fire-resistance time of the *reference* (ISO) scenario that is obtained using ultimate available rotation values which do not contain initial imperfections. In this case, it is interesting to notice that the reduction of the fire-resistance time is considerable for all the amplitudes of initial imperfection that are studied and lies between 14% (for the design earthquake) and 24% when the scale factor 1.75 is used for the escalation of the earthquake intensity. In the second case, the mean value of the fire-resistance time is compared with the fire-resistance time of the *reference* (ISO) scenario that is obtained using ultimate available rotation values which take into account initial imperfections. In this case the comparison is conducted with respect to equal values of initial imperfections. The reduction of the fire-resistance time of the damaged structure with respect to the value that corresponds to the structure that is not damaged due to earthquake is between the 2% and 7% and this magnitude increases as the amplitude of initial imperfection is enlarged.

Table 7 Fire-resistance of the frame structure in time domain (sec) for the ISO-FAE scenarios for different amplitude of imperfections - Comparison with the *reference* ISO-fire *reference* scenario

Amplitude of initial imperfections 0.5mm			
Reference ISO scenario			
Perfect model	1563		
Imperfect model	1388		
ISO-FAE scenarios			
Accelerogram	Seismic action level		
	S.F. 1	S.F. 1.25	S.F. 1.50	S.F. 1.75
290xa	1337	1336	1319	-
293ya	1355	1335	1321	1306
612xa	1339	1316	1291	-
1726xa	1358	1324	1304	-
1726ya	1343	1329	1311	1302
5850xa	1346	1333	1319	1316
6142ya	1371	1347	1337	1320
Mean time	**1350**	**1331**	**1315**	**1311**
Reduction[1]	**13.64%**	**14.82%**	**15.89%**	**16.12%**
Reduction[2]	**2.75%**	**4.08%**	**5.29%**	**5.55%**

Table 7 Continued

Amplitude of initial imperfections 2 mm			
Reference ISO scenario			
Prefect model	1563		
Imprefect model	1323		
ISO-FAE scenarios			
Accelerogram	Seismic action level		
	S.F. 1	S.F. 1.25	S.F. 1.50	S.F. 1.75
290xa	1288	1282	1258	-
293ya	1298	1285	1263	1246
612xa	1288	1253	1227	-
1726xa	1300	1269	1244	-
1726ya	1294	1275	1247	1239
5850xa	1296	1283	1260	1253
6142ya	1312	1297	1283	1259
Mean time	**1297**	**1278**	**1255**	**1249**
Reduction[1]	**17.05%**	**18.25%**	**19.73%**	**20.07%**
Reduction[2]	**2.00%**	**3.42%**	**5.17%**	**5.57%**
Amplitude of initial imperfections 5 mm			
Reference ISO scenario			
Prefect model	1563		
Imperfect model	1291		
ISO-FAE scenarios			
Accelerogram	Seismic action level		
	S.F. 1	S.F. 1.25	S.F. 1.50	S.F. 1.75
290xa	1245	1244	1210	-
293ya	1264	1246	1218	1189
612xa	1249	1205	1133	-
1726xa	1262	1228	1186	-
1726ya	1253	1230	1195	1177
5850xa	1276	1243	1214	1205
6142ya	1258	1257	1242	1216
Mean time	**1258**	**1236**	**1200**	**1197**
Reduction[1]	**19.51%**	**20.91%**	**23.24%**	**23.43%**
Reduction[2]	**2.55%**	**4.25%**	**7.07%**	**7.30%**

[1]Reduction with respect to the fire resistance of the *reference* scenario considering ultimate available rotation values that do not take into account initial imperfections

[2]Reduction with respect to the fire resistance of the *reference* scenario considering ultimate available rotation values that take into account initial imperfections
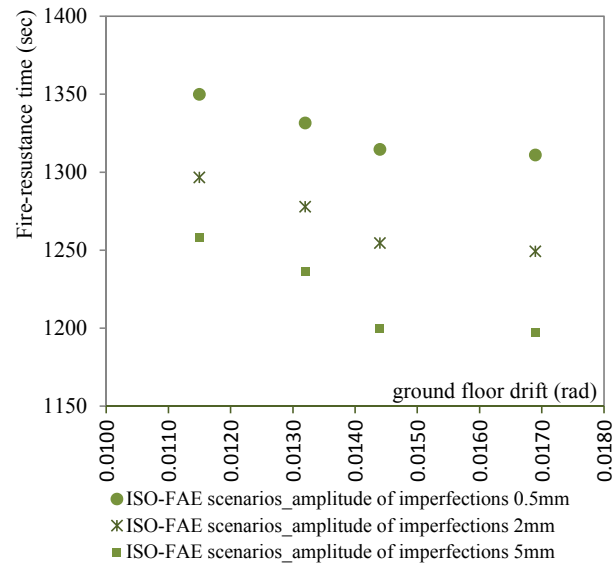
Fig. 11 Comparison of fire-resistance time for ISO and Natural FAE scenarios (in ISO-fire time)

Fig. 11 summarizes the results, concerning the fire-resistance of the structural system in time domain. The fire-resistance is plotted against the average inter-storey drift of the ground floor that is induced in the structural system during the corresponding earthquake excitation. It is noted that the increase of the average drift corresponds to more severe seismic actions. It can be concluded that as the earthquake return period increases and, subsequently, the earthquake becomes more severe, the fire-resistance of the structural system is slightly reduced. Moreover, for the more rare earthquake actions it remains almost constant (comparison between the fire-resistance time that corresponds to drift 0.0169 and 0.0211). This remark holds for all the amplitudes of initial imperfections that are studied. The reduction of the fire-resistance becomes more important as the amplitude of the initial imperfections increases.

10. Conclusions

In this study the fire-resistance of the structural system is calculated, in time domain, for both the *reference* and the FAE scenarios. The calculations use the rotational limits based on the ductility of heated structural members. It is concluded that the upper limit of the reduction of the fire-resistance of the structure for the FAE loading, with respect to the fire resistance of the *reference* scenario (considering ultimate available rotation values that do not take into account initial imperfections) is approximately 25%. The reduction is important and this indicates that the structural system should be re-designed in order to take into account the FAE loading. Finally, it is noted that the calculation of the fire-resistance of the structural system, for both fire and FAE scenarios, should be based on ductility ultimate available rotation values that take into account the effect of the initial imperfection. In the case of the FAE loading, it is important the ultimate available rotation values to be dependent on the 'level of the damage' that is induced in the structural system due to the seismic action.

References

Cosenza, E. and Manfredi, G. (2000), "Damage indices and damage measures", *Prog. Struct. Eng. Mater.*, **2**(1), 50-59.

Della Corte, G., Landolfo, R. and Mazzolani, F.M. (2003), "Post-earthquake fire resistance of moment resisting steel frames", *Fire Safety J.*, **38**(7), 593-612.

Eurocode 8 (2004), *Design of structures for earthquake resistance* - Part 1: General rules seismic actions and rules for buildings, Brussels.

Eurocode 3 (2003), *Design of steel structures*- Part 1-2: General Rules - Structural fire design, Brussels.

Eurocode 1 (2002), *Actions on structures exposed to fire* - Part 1-2. General actions - structural fire design, Brussels.

Eurocode (2006), *Basis of structural design*, Brussels.

Faggiano, B., Espoto, M., Mazzolani, F.M. and Landolfo, R. (2007), "Fire analysis of steel portal frames damaged after earthquake according to performance based design", *Urban Habitat Constructions under Catastrophic Events, Cost C26, Workshop*, Prague, Czech Republic.

Faggiano, B., Espoto, M., Zaharia, R. and Pintea, D. (2008), "Structural analysis in case of fire after earthquake", *Urban Habitat Constructions under Catastrophic Events, Cost Action C26*, Malta University.

Faggiano, B. and Mazzolani F.M. (2011), "Fire after earthquake robustness evaluation and design: Application to steel structures", *Steel Constr. Des. Res.*, **4**(3), 183-187.

Iervolino, I., Maddaloni, G. and Cosenza, E. (2008), "Eurocode 8 compliant real record sets for seismic analysis of structures", *J. Earthq. Eng.*, **12**(1), 54-90.

Kappos, A. (1997), "Seismic damage indices for RC buildings: evaluation of concepts and procedures", *Prog. Struct. Eng. Mater.*, **1**(1), 78-87.

Keller, W.J. (2012), "Thermomechanical response of steel moment-frame beam-column connections during post-earthquake Fire Exposure", Ph. D Dissertation, Lehigh University, Bethlehem, Pennsylvania.

Keller, W. and Pessiki, S. (2012), "Effect of earthquake-induced damage to spray-applied fire-resistive insulation on the response of steel moment-frame beam-column connections during fire exposure", *J. Fire Protection Eng.*, **22**(4), 271-299.

Kodur, V. and Dwaikat, M. (2009), "Response of steel beam-columns exposed to fire", *Eng. Struct.*, **31**(2), 369-379.

Lee, S., Davidson, R., Ohnishi, N. and Scawthorn, C. (2008), "Fire following earthquake-reviewing the State-of-the-Art of modeling", *Earthq. Spectra*, **24**(4), 933-967.

MSC Software Corporation (2010), *MSC Marc Volume A: Theory and User Information*, USA.

Pantousa, D. and Mistakidis, E. (2014), "Rotational capacity of damaged and undamaged steel I-beams at elevated temperatures", *Proceedings of the seventh International Conference EUROSTEEL*, Naples.

Scawthorn, C., Eidinger, J.M. and Schiff, A. (2005), "Fire following earthquake", Technical Council on Lifeline Earthquake Engineering Monograph No. **26**, 345, American Society of Civil Engineers, Reston.

Vamvatsikos, D. and Cornell, C.A. (2002), "Incremental dynamic analysis", *Earthq. Eng. Struct. Dyn.*, **31**(3), 491-514.

Yassin, H., Iqbal, F., Bagchi, A. and Kodur, V.K.R. (2008), "Assessment of post-earthquake fire performance of steel-frame buildings", *Proceedings of 14th World Conference on Earthquake Engineering*, Beijing.

Zaharia, R., Pintea, D. and Dubina, D. (2007), "Fire analysis and design of a composite steel-concrete structure", *Steel Compos. Struct.*, Taylor & Francis Group London.

Zaharia, R., Pintea, D. and Dubina, D. (2008) "Fire after earthquake- a natural fire approach", *Proceedings of the fifth International Conference EUROSTEEL*, Austria.

Zaharia, R., Pintea, D. and Dubina, D. (2009), "Fire analysis of structures in seismic areas", *Proceedings of the International Conference on Application of Structural Fire Engineering*, Prague, Czech Republic.

Zaharia, R. and Pintea, D. (2009), "Fire after earthquake analysis of steel moment resisting frames", *Int. J.*

Steel Struct., **9**(4), 275-284.
Zhao S. (2010), "GisFFE-an integrated software system for the dynamic simulation of fires following an earthquake based on GIS", *Fire Safety J.*, **45**(2), 83-97.

SA